Regulation of sexually dimorphic abdominal courtship behaviors in Drosophila by the *Tlx*/*tailless*-like nuclear receptor, *Dissatisfaction*

Julia C. Duckhorn[1], Jessica Cande[2], Mary C. Metkus[1], Hyeop Song[1], Sofia Altamirano[1], David L. Stern[2] & Troy R. Shirangi[1,3]

[1] Villanova University, Department of Biology, 800 Lancaster Ave, Villanova, PA 19085

[2] Janelia Research Campus, Howard Hughes Medical Institute, 19700 Helix Drive, Ashburn, VA 20147

[3] Correspondence: troy.shirangi@villanova.edu

Abstract

Sexually dimorphic courtship behaviors in *Drosophila melanogaster* develop from the activity of the sexual differentiation genes, *doublesex* (*dsx*) and *fruitless* (*fru*), functioning with other regulatory factors that have received little attention. The *dissatisfaction* gene (*dsf*) encodes an orphan nuclear receptor homologous to vertebrate *Tlx* and Drosophila *tailless* that is critical for the development of several aspects of female- and male-specific sexual behaviors. Here, we report the pattern of *dsf* expression in the central nervous system and show that the activity of sexually dimorphic abdominal interneurons that co-express *dsf* and *dsx* is necessary and sufficient for vaginal plate opening in virgin females and abdominal curling in males during courtship. We find that *dsf* activity results in different neuroanatomical outcomes in females and males, promoting and suppressing, respectively, female development and function of these neurons depending upon the sexual state of *dsx* expression. We posit that *dsf* and *dsx* interact to specify sex differences in the neural circuitry for dimorphic abdominal behaviors.

Introduction

The neural circuitry required for sex-specific behaviors in *Drosophila melanogaster* is currently understood to be specified during development by transcriptional regulators encoded by the *doublesex* (*dsx*) and *fruitless* (*fru*) genes [1]. The male isoforms of *dsx* and *fru* direct the differentiation of neurons in the adult male central nervous system that are required for performance of male courtship behaviors [2–6]. Conversely, the female-specific isoform of the *dsx* gene together with the absence of male-specific *fru* build the neural pathways that direct female-specific sexual behaviors [3,6–9].

Although *dsx* and *fru* are indispensable for sexual differentiation of the *Drosophila* nervous system, they act together with other regulatory genes that have been less well studied [10,11]. The *dissatisfaction* gene (*dsf*), for instance, which encodes an orphan nuclear receptor homologous to vertebrate *Tlx* and Drosophila *tailless*, is required for several aspects of female- and male-specific reproductive behaviors [12,13]. Females homozygous for null mutations of *dsf* rarely mate with courting males, and, if fertilized, are unable to lay eggs despite being able to ovulate [12]. Males mutant for *dsf* court females and males indiscriminately and are delayed in copulating with females at least in part due to deficits in abdominal bending during copulation attempts [12]. The *dsf* gene was first identified over twenty years ago, yet where and when *dsf* is precisely expressed in the Drosophila nervous system, which *dsf*-expressing neurons matter for courtship behavior, and how *dsf* contributes to the sexual differentiation of the nervous system are not known.

Here, we report *dsf*'s spatial and temporal expression in the central nervous system and discover a small group of sexually dimorphic *dsf* and *dsx* co-expressing interneurons in the abdominal ganglion called the DDAG neurons. Females and males have approximately twelve and three DDAG neurons per side, respectively, that exhibit sexually dimorphic projection patterns in the ventral nerve cord. Optogenetic activation and neural silencing experiments demonstrate that the DDAG neurons contribute to vaginal plate opening in females and abdominal curling in males during courtship. In females, *dsf* promotes the presence of female-specific DDAG neurons and the development of vaginal plate opening behavior. *dsf* acts in an opposite

manner in males, suppressing the development of a female-like DDAG neuron. Optogenetic activation of artificially induced female-like DDAG neurons in males drives an abdominal behavior in males that imitates vaginal plate opening in females. We show that *dsf* promotes or suppresses female-like development and function of the DDAG neurons depending upon the expression of the male isoform of *dsx*. Taken together, our results illustrate how the *dsf* gene regulates the development and function of sexually dimorphic neurons that mediate sex-specific abdominal behaviors.

Results

Expression of *dsf* in the Drosophila central nervous system

In a previous study [13], *dsf* expression in the Drosophila central nervous system (CNS) was detected by *in situ* hybridization in a small number of neurons located primarily in anterior regions of the pupal and adult protocerebrum. We reexamined *dsf* mRNA expression in the adult CNS by *in situ* hybridization chain reaction (HCR), a robust, quantitative, and sensitive method to detect mRNAs in whole-mounted tissues [14–16]. Using HCR probe-sets directed against *dsf*, we observed *dsf* mRNAs in the Canton S CNS in substantially more cells than originally reported (Figure 1a, b). In the brain, *dsf* expression was found in several broadly distributed clusters of cells located mostly on the anterior side, dorsal and ventral to the foramen of the esophagus. Hybridization signals were also detected in a few cells in the thoracic and abdominal neuromeres of the ventral nerve cord (VNC). The intensities and distributions of hybridization signals appeared similar between the sexes, and hybridization signals were not detected in flies null for the *dsf* gene (Figure 1c, d).

To characterize the identity, anatomy, and function of *dsf*-expressing cells, we used CRISPR/Cas9-mediated homology-directed repair to insert the Gal4 transcriptional activator from yeast into the *dsf* translational start codon, generating a dsf^{Gal4} allele (Figure 2a). Insertion of Gal4 deleted all coding sequences within *dsf*'s first exon and the exon's 5′ splice site, thereby creating a loss-of-function allele. We assessed whether dsf^{Gal4} reproduces the endogenous pattern of *dsf* transcripts by sequentially applying *in situ* HCR and immunohistochemistry to adult

82 CNS tissues from flies heterozygous for *dsf*^{Gal4} and carrying *UAS-nls::gfp* to simultaneously de-
tect *dsf* transcripts and GFP expression. We found an almost perfect overlap of the two markers
84 in the adult brain and VNC of females and males (Figure 2b, c). All cells in the adult CNS la-
beled by *dsf*^{Gal4} co-expressed the pan-neuronal marker, ELAV, confirming that the *dsf*-expressing
86 cells are neuronal (Supplemental Figure 1a–d).

We categorized *dsf*-expressing neurons as belonging to specific clusters of neurons and
88 used standardized nomenclature [17,18] to assign names to each neuronal group based on their
location in the cell body rind of the brain and VNC (Figure 2d–f). *dsf*-expressing neurons in the
90 brain occur in twelve discernible groups on the left and right sides. Eight of the neuronal
groups are in the supraesophageal zone of the brain and four are present in the subesophageal
92 zone. All twelve groups of neurons are present in both sexes, but some groups (*i.e.*, rSMPma,
rALad, and rALv) exhibit notable differences in neuron number between the sexes (Figure 2f).
94 The difference in the number of *dsf*-expressing neurons in female versus male VNCs results en-
tirely from a difference in the number of *dsf*-expressing neurons within the abdominal ganglion.

96 When driving a membrane-targeted GFP, *dsf*^{Gal4} labeled many different nerve bundles
and synaptic neuropils present mostly on the posterior side of the adult brain and in the VNC
98 (Figure 2g, h). No obvious sex differences in the projection patterns of *dsf*-expressing neurons
were observed in the adult CNS. *dsf*^{Gal4} also labeled subsets of neurons in the late 3rd instar larval
100 and pupal (Supplemental Figure 1e–j) CNS. We did not detect *dsf*^{Gal4} expression in peripheral
sensory neurons or in motoneurons at any stage that we examined. We conclude that *dsf* is ex-
102 pressed in several subsets of neurons broadly distributed across the female and male CNS of
adult, pupal, and larval stages, and that Gal4 expression from the *dsf*^{Gal4} allele faithfully recapit-
104 ulates the *dsf* wild-type expression pattern.

106 **A sexually dimorphic group of *dsf* and *dsx* co-expressing neurons contribute to female- and male-specific abdominal courtship behaviors**

108 *dsf* contributes to courtship behaviors [12] that are also influenced by *dsx* gene function
or *dsx*-expressing neurons [6–8,19]. We reasoned that *dsf*-expressing neurons relevant for some
110 courtship behaviors may co-express *dsx*. We therefore genetically intersected *dsf*^{Gal4} with *dsx*^{LexA}

[19], which expresses *LexA::p65* in all *dsx*-expressing cells. dsx^{LexA} was used to drive a *LexAop*-controlled Flp recombinase, which excised a transcriptional stop cassette from an upstream activating sequence (UAS)-myr::GFP transgene driven by dsf^{Gal4}. This intersection ($dsf^{Gal4} \cap dsx^{LexA}$) labeled a small group of sexually dimorphic interneurons (hereafter referred to as the *dsf-dsx* abdominal ganglion, or DDAG, neurons) in the abdominal ganglion of both sexes (Figure 3a, b). Males have three DDAG neurons on the left and right sides that arborize locally within the abdominal neuropil and whose cell bodies are located on the ventral side of the VNC. Females appear to share these neurons and also possess approximately nine female-specific interneurons, four of which are located on the dorsal side of the VNC. The DDAG neurons of females arborize extensively within the abdominal ganglion, and some neurons extend neurites in the anteriorly to innervate all three thoracic neuropils. The intersection between dsf^{Gal4} and dsx^{LexA} does not appear to label any other cells in the brain or VNC.

To determine whether the DDAG neurons contribute to courtship behaviors, the $dsf^{Gal4} \cap dsx^{LexA}$ intersection was used to target the expression of the red light-gated cation channel *CsChrimson* [20] to activate the DDAG neurons. When stimulated with red light, $dsf^{Gal4} \cap dsx^{LexA}$ > *CsChrimson* virgin females adjusted the posture and length of their abdomen and opened their vaginal plates, partially exposing their ovipositor (Figure 4a; Supplemental Video 1). Virgin females normally open their vaginal plates if they are receptive to courting males [21,22]. In contrast, mated females signal their unwillingness to mate by extruding their ovipositor [21,23,24]. The length of the female's abdomen increases during both behaviors, but by a greater amount during an ovipositor extrusion (Figure 4b). To confirm that photoactivation of the DDAG neurons in females triggered an opening of the vaginal plates and not an ovipositor extrusion, we measured the change in abdomen length before and after photoactivation and compared it to the change in abdomen length when virgin females open their vaginal plates or when mated females extrude their ovipositor. Optogenetic activation of the DDAG neurons in females induced a change in abdomen length more similar to that measured when virgin females open their vaginal plates during courtship than when mated females extrude their ovipositor (Figure 4b). Females opened their vaginal plates immediately and only during photoactivation of the DDAG

neurons (Figure 4c). We observed quantitatively similar behavior across a range of stimulus in-
140 tensities (Figure 4d, e).

We next tested whether the activity of the DDAG neurons is required for vaginal plate
142 opening in virgin females. We used *dsf*^{Gal4} ∩ *dsx*^{LexA} to drive the expression of tetanus neurotoxin light chain (*tnt.e*) [25] to suppress the function of the DDAG neurons in females. Compared to a
144 control that expressed an inactive form of the neurotoxin (*tnt.QA*), virgin females that expressed *tnt.e* in the DDAG neurons mated infrequently with courting males (Figure 4f) despite being
146 vigorously courted (Figure 4g), and exhibited a marked reduction in the frequency of vaginal plate opening during courtship (Figure 4h). Females with inhibited DDAG neurons that eventu-
148 ally mated produced and released eggs into the oviduct (not shown), but failed to lay any eggs and eventually appeared gravid. These results demonstrate that the DDAG neurons in virgin
150 females contribute to vaginal plate opening and female receptivity, and to later steps of egg laying.

152 In males, we observed that photoactivation of the DDAG neurons induced abdomen bending (Figure 5a–c; Supplemental Video 2). During *Drosophila* courtship, males attempt to
154 copulate with females by curling their abdomen ventrally by ~180º to achieve contact between genitalia. Males with inhibited DDAG neurons (*dsf*^{Gal4} ∩ *dsx*^{LexA} > *tnt.e*) actively courted Canton S
156 virgin females, but were strongly reduced in successful mating rates relative to control (*dsf*^{Gal4} ∩ *dsx*^{LexA} > *tnt.QA*) males (Figure 5d, e). Additionally, in comparison with controls, males with in-
158 hibited DDAG neurons showed markedly reduced frequency of abdomen bending per minute of active courtship (Figure 5f). We conclude that the DDAG neurons of females and males in-
160 fluence sex-specific abdominal behaviors during courtship.

162 **Sexually dimorphic anatomy and function of the DDAG neurons results from *dsx*M-mediated defeminization**

164 We next sought to determine how the dimorphic development of the DDAG neurons is genetically regulated. *dsf*^{Gal4} ∩ *dsx*^{LexA} > *myr::gfp* was used to visualize the DDAG neurons as be-
166 fore, but now we used a validated UAS-regulated *dsx* ShmiR [26,27] to deplete *dsx* transcripts in

dsf-expressing cells of both sexes. Depletion of male-specific *dsx* (*dsx*M) transcripts in *dsf*-expressing cells resulted in a near complete anatomical feminization of the DDAG neurons in males (Figure 6a–e); males gained approximately nine interneurons with an arborization pattern similar to that of females. Knock-down of female-specific *dsx* (*dsx*F) transcripts, however, did not result in any obvious changes in DDAG anatomy (Figure 6a–e). These results indicate that sex differences in the DDAG neurons require *dsx*M-mediated defeminization, whereby *dsx*M removes a set of neurons normally found in females, possibly through regulation of programmed cell death. In the absence of sexual differentiation (*i.e.*, without *dsx* function), the DDAG neurons develop monomorphically but in the likeness of female DDAG neurons.

To determine whether the depletion of *dsx* activity influences the function of the DDAG neurons, we photoactivated the DDAG neurons in females and males that expressed *dsx-ShmiR* driven by dsf^{Gal4}. Photoactivation triggered the opening of the vaginal plates in females, similar to control females that lacked the *UAS-dsx-ShmiR* transgene (Figure 6j, k; Supplemental Video 3), consistent with the absence of an obvious neuroanatomical phenotype in the DDAG neurons of dsf^{Gal4} > *UAS-dsx-ShmiR* females. In contrast, photoactivation failed to induce abdomen curling in males, but instead triggered a novel behavior in which the males extended their abdomen and extruded their terminalia (*i.e.*, the terminal appendage consisting of genital and anal structures) during illumination (Figure 6l, m; Supplemental Video 4). This behavior imitated vaginal plate opening behaviors of virgin females during courtship.

To confirm that these optogenetically induced terminalia extrusions result from a feminization of the DDAG neurons, we constructed $dsf^{Gal4} \cap dsx^{LexA}$ > *CsChrimson* males that included a UAS-regulated female-specific *transformer* (*tra*F) transgene [28], as an alternative strategy to feminize the DDAG neurons (Supplemental Figure 2). When stimulated with red light, the DDAG neurons of dsf^{Gal4} > *UAS-traF* males triggered extrusions of the terminalia at levels similar to dsf^{Gal4} > *UAS-dsx-ShmiR* males (Supplemental Figure 2). Taken together, our data indicate that *dsx*M regulates the sexually dimorphic development of the DDAG neurons in part by defeminizing the anatomy and function of the DDAG neurons. Although our results do not support a role for *dsx*F, we cannot rule out the possibility that *dsx*F contributes to aspects of DDAG sexual development undetected in our analyses.

196

dsf exerts opposite effects on the development and function of the DDAG neurons in females

198 **and males depending upon the expression of _dsx_M**

Females carrying loss-of-function mutations in *dsf* mate infrequently with courting

200 males, and *dsf* mutant males exhibit reduced copulation rates that correlate with abnormalities in abdomen bending during courtship [12]. Our results demonstrate that the DDAG neurons

202 influence most courtship traits altered in *dsf* mutants. To determine whether *dsf* gene function is required specifically in the DDAG neurons for wild type abdominal courtship behaviors, we de-

204 pleted *dsf* neurons using a $dsx^{Gal4(\Delta 2)}$ [29] and a validated UAS-controlled *dsf-ShmiR*. Compared to controls that carried only either the Gal4 or UAS transgenes, $dsx^{Gal4(\Delta 2)}$ > *UAS-dsf-ShmiR* virgin

206 females mated infrequently with courting Canton S males, displayed a reduction in the frequency of vaginal plate opening during active male courtship (Figure 4i, j), and retained their

208 eggs (not shown). Depletion of *dsf* transcripts in the DDAG neurons of males resulted in reduced mating rates with Canton S virgin females and a reduced frequency of abdomen bends

210 during courtship (Figure 5g, h). These data suggest that *dsf* contributes to female and male courtship behaviors at least in part through *dsf* activity in the DDAG neurons.

212 We next asked whether *dsf* influences the development of the DDAG neurons. We used $dsf^{Gal4} \cap dsx^{LexA}$ > *myr::gfp* to visualize and compare the DDAG neurons of a *dsf* loss-of-function

214 mutant (dsf^{Gal4}/dsf^{Del}) with a heterozygous control (dsf^{Gal4}/+). Control females have approximately twelve bilaterally paired DDAG neurons on the left and right sides of the VNC (Figure 6a, b),

216 about five of which are lost in the absence of *dsf* function (Figure 6a, f). The lost neurons included some of the female-specific, dorsal DDAG neurons. Additionally, the neurites of the

218 DDAG neurons that normally project to the thoracic ganglia in control females were substantially reduced in *dsf* mutant females (Figure 6f). In contrast, the loss of *dsf* in males resulted in a

220 gain of a single bilateral pair of DDAG neurons in the dorsal abdominal ganglion (Figure 6a, g). This neuron extends a neurite shaped like a handlebar moustache anteriorly to innervate the

222 third thoracic neuropil (Figure 6g). Both the neuron's location on the dorsal side and its gross projection pattern are similar to DDAG neurons found in females, suggesting that the loss of *dsf*

224 activity in males may have partially feminized the anatomy of DDAG neurons. Thus, *dsf* function promotes development of some DDAG neurons in females and suppresses development of
226 similar (perhaps homologous) neurons in males.

To determine how the loss of *dsf* activity may affect the function of the DDAG neurons,
228 we photoactivated the DDAG neurons in *dsf* mutant females and males ($dsf^{Gal4}/dsf^{Del} \cap dsx^{LexA}$ > *CsChrimson*). In contrast to control ($dsf^{Gal4} \cap dsx^{LexA}$ > *CsChrimson*) flies, photoactivation of the
230 DDAG neurons in *dsf* mutants did not elicit vaginal plate opening in females (Figure 6k; Supplemental Video 5) nor abdominal curling in males (Figure 5c), but *dsf* mutant males extruded
232 their terminalia during bouts of illumination (Figure 6m; Supplemental Video 6). The fraction of time *dsf* mutant males extruded their terminalia during an illumination bout was variable, and
234 some *dsf* mutant males extruded their terminalia even after the illumination period had ended (Figure 6m). Our results suggest that *dsf* promotes female-type development of the DDAG neu-
236 rons and vaginal plate opening behavior in females, but functions in an opposite manner in males, suppressing the presence of a single female-like DDAG neuron whose activity is associ-
238 ated with a feminized abdominal behavior.

These observations led us to consider the possibility that *dsf* promotes or suppresses fe-
240 male-type development and function of the DDAG neurons depending on the neurons' sexual identity. In the absence of *dsx* expression (and hence sexual differentiation), the DDAG neurons
242 develop similarly in both sexes and as they do normally in females (Figure 6a). We thus posited that in the context of reduced *dsx* activity, *dsf* would influence DDAG development similarly in
244 females and males, but as it normally does in females, promoting the presence of female-specific neurons that contribute to feminized abdominal behaviors. Consistent with these expectations,
246 removal of *dsf* activity in flies with reduced *dsx* expression resulted in a loss of about five DDAG neurons in both sexes (Figure 6a). Moreover, these flies opened their vaginal plates and
248 extruded their terminalia at reduced levels upon photoactivation of the DDAG neurons relative to dsf^{Gal4} > *UAS-dsx-ShmiR* control flies (Figure 6k, m).

250 Taken all together, our results suggest that *dsf* acts as both a 'pro-female' and 'anti-female' factor for DDAG development depending upon the expression of *dsx*M. When *dsx*M is ab-

sent, as in females, *dsf* promotes the presence of female-specific DDAG neurons that likely contribute to vaginal plate opening behavior in females during courtship. However, when DsxM is present, as in males, *dsf* defeminizes the DDAG neurons, suppressing the presence of a female-like DDAG neuron.

Discussion

We have discovered a sexually dimorphic group of *dsf* and *dsx* co-expressing abdominal interneurons called the DDAG neurons that contribute to vaginal plate opening in virgin females and abdominal curling in males during courtship. Recently, the neural circuit mechanisms in the brain that mediate female receptivity and the opening of the vaginal plates in virgin females have been characterized [22]. Female-specific DDAG neurons may function in the circuits downstream of descending neurons in the brain that trigger the opening of the vaginal plates during courtship. In females, *dsf* promotes the development of female-type DDAG neurons that regulate the opening of the vaginal plates, but acts in an opposite manner in males, suppressing the development of female-like DDAG neurons. Whether *dsf* promotes or suppresses female-like DDAG development appears to depend upon the expression of *dsx*. Several groups of *dsf*-expressing, *dsx*-non-expressing neurons in the brain also exhibit sex differences in cell number. These neurons likely co-express *fru* and may contribute to other sex-specific behaviors altered in *dsf* mutants.

Dsf encodes an orphan nuclear receptor homologous to the Drosophila *tailless* (*tll*) and vertebrate *Tlx* genes [13]. In mice, *Tlx* is expressed in all adult neural stem cells [30], where it functions to maintain the cells in a proliferative state [31,32]. Similarly, in Drosophila, *tll* regulates the maintenance and proliferation of most neural progenitors in the protocerebrum [33]. At the developmental stages we examined, dsf^{Gal4} expression in the ventral nerve cord was observed exclusively in mature neurons and not in any neuronal progenitors. This suggest that *dsf* may regulate neuron number post-mitotically, directing the survival or death of female-specific DDAG neurons depending upon the sex of the fly.

The loss of *dsf* in otherwise wild-type flies results in a loss of female-specific DDAG neurons in females and a gain of a female-like DDAG neuron in males. However, in the context of

reduced *dsx* activity, the loss of *dsf* causes a sexually monomorphic loss of DDAG neurons.
282 Thus, *dsf* contributes to the development of the DDAG neurons differently in females and males depending upon the expression of *dsx*. How the expression of *dsx* may influence *dsf* activity is
284 not known. As the neural circuits for courtship develop during pupal life, a subset of *dsf*-expressing neurons in the abdominal ganglion of both sexes gain *dsx* expression (S. Altamirano &
286 T. Shirangi, unpublished results). We hypothesize that the expression of *dsx*M in males then directs the cell death of female-specific DDAG neurons in part by antagonizing *dsf*'s function in
288 promoting the survival of some female-specific DDAG neurons. How might DSX-M and DSF interact molecularly? Although nuclear receptors including *dsf* generally act as transcriptional
290 repressors, some can also function as activators upon binding to a cognate ligand [34–36] or after post-translational modification [37]. Thus, in one scenario, the expression of DSX-M could
292 sex-specifically impact DSF activity by regulating the generation of DSF's ligand (if it has one) or the occurrence of a post-translational modification. Alternatively (but not exclusively), ex-
294 pression of *dsf* may be directly regulated by DSX proteins. Consistent with this scenario, an *in vivo* genome-wide study of DSX occupancy identified *dsf* as a putative DSX target gene [38].
296 Moreover, an intronic regulatory fragment from *dsf* containing the sites occupied by DSX drives reporter expression in female-specific DDAG neurons (J. Diamandi, J. Duckhorn, J. Cande & T.
298 Shirangi, unpublished results). It is therefore possible that DSX-M represses *dsf* expression in a subset of DDAG neurons that contribute to vaginal plate opening behavior, thereby directing
300 the removal of the neurons in males but not females.

Experimental Procedures

Fly stocks

Fly stocks were maintained on standard cornmeal and molasses food at 25°C. The stocks used in this study include the following: *Canton S*, w^{1118}, *Df(2L)ED284/CyO* (BDSC 8040), *Df(2L)BSC183/CyO* (BDSC 9611), *pJFRC32-10XUAS-IVS-nlsGFP* (attP40), *pJFRC29-10XUAS-IVS-myr::GFP-p10* (attP2), $dsx^{\text{LexA::p65}}$ [19], *pJFRC79-8XLexAop2-FlpL* (attP40), *pJFRC41-10XUAS-FRT>STOP>FRT-myr::gfp* (su(Hw)attP1), *20XUAS-FRT>STOP>FRT-CsChrimson-mVenus* (VK5), *UAS-FRT>STOP>FRT-tnt.e* and *UAS-FRT>STOP>FRT-tnt.QA*, $dsx^{\text{Gal4}(\Delta 2)}$ [29], *P{y[+t7.7] v[+t1.8]=TRiP.GLV21010}attP2* (*i.e.*, *UAS-dsx-ShmiR*; obtained from *Drosophila* Transgenic RNAi Project at Harvard Medical School), and *UAS-traF* (BDSC 4590). *UAS-dsf-ShmiR* (attP2) was created according to protocols described in Haley *et al.* [39]. Two stem-loops targeting sequences in *dsf*'s fourth exon were placed into an intron from the *ftz* gene upstream of a cDNA encoding *nls::gfp*. This construct was cloned into the BglII/XbaI sites in pMUH.

Construction of dsx^{Gal4} and dsf^{Del} alleles

The dsf^{Gal4} allele was created using CRISPR/Cas9-mediated homology-directed repair to precisely introduce Gal4 into *dsf*'s start codon in exon 1. The Gal4 cDNA/hsp70 yeast terminator sequence was amplified from pBPGuW (Addgene). A donor plasmid was generated by combining a 1,050-bp left homology arm, the Gal4/terminator sequence, 3XP3::DsRed marker (with an inverted orientation), a 1,149-bp right homology arm, and a 1.8-kb backbone using Gibson Assembly [40]. Guide RNAs (5′-CATCAACGGAAAATGGGCAC-3′ and 5′-ATACTTCCATCAACGGAAAA-3′) were cloned into the pCFD4 plasmid [41]. The donor and pCFD4 plasmids, *in vitro* transcribed codon optimized Cas9 mRNA, and a lig4 siRNA were co-injected into w^{1118} embryos. The dsf^{Del} allele was created using an identical strategy except the Gal4/terminator sequence was excluded from the donor plasmid.

in situ hybridization chain reaction and immunohistochemistry

Nervous systems were dissected in 1X PBS, fixed in 4% paraformaldehyde buffered in PBS for 35 min at room temperature, and rinsed and washed in PBT (PBS with 1% Triton X-100). *in situ*

330 hybridization chain reaction experiments were conducted as in described in using HCR probe-
sets (*dsf*-B1, Lot #: PRF061) and hairpins (B1h1-AF488, B1h2-AF488) synthesized by Molecular
332 Instruments™. We used a probe-set size of 20. After dissection and fixation, the tissues were
pre-hybridized in prewarmed probe hybridization buffer (Molecular Instruments™) for 30
334 minutes at 37°C and incubated with HCR probes in probe hybridization buffer overnight at
37°C. Tissues were washed the next day in prewarmed probe wash buffer four times, 15
336 minutes each at 37°C, and washed in 5X SSCT (UltraPure 20X SSC Buffer, Invitrogen #15557044,
diluted in water) three times, 5 minutes at room temperature. Tissues were pre-amplified in am-
338 plification buffer (Molecular Instruments™) for 30 minutes at room temperature and incubated
with snap-cooled HCR hairpins in amplification buffer overnight at room temperature, pro-
340 tected from light. Tissues were then washed with 5X SSCT at room temperature twice for 5
minutes, twice for 30 minutes, and once for 5 minutes before being mounted in VECTASHIELD
342 (Vector Laboratories, H-100) or proceeding with an immunohistochemistry protocol. Immuno-
histochemistry was performed as described in [27]. Nervous systems were incubated with pri-
344 mary antibodies in PBT overnight at 4°C. Tissues were washed in PBT at room temperature for
several hours and incubated overnight with secondary antibodies at 4°C. Tissues were washed
346 in PBT for several hours at room temperature, mounted onto poly-lysine coated coverslips, de-
hydrated through an ethanol series, cleared in xylenes, and mounted in DPX (Sigma-Aldrich)
348 on a slide. If immunohistochemistry followed *in situ* HCR, nervous systems were mounted in
VECTASHIELD. The following antibodies were used: rabbit anti-GFP (Invitrogen #A11122;
350 1:1,000), rat anti-DN-cadherin (DN-Ex #8, Developmental Studies Hybridoma Bank; 1:50),
mouse anti-Elav (9F8A9, Developmental Studies Hybridoma Bank; 1:20), AF-647 goat anti-rat
352 (Invitrogen #A21247; 1:500), Fluorescein (FITC)-conjugated donkey anti-rabbit (Jackson Immu-
noResearch; 1:500), AF-568 goat anti-mouse (Invitrogen #A11004; 1:500). Tissues were imaged
354 on a Leica SP8 confocal microscope at 40X with optical sections at 0.3 μm intervals.

356 **Behavior and optogenetic assays**

Newly eclosed flies were collected under CO_2 and aged for 7–10 days at 25°C and ~50% humid-
358 ity in a 12-hr light/dark cycle unless otherwise noted. Virgin females and males used in optoge-
netic assays were raised in darkness at 25°C on food containing 0.2 mM all-*trans*-Retinal (Sigma-
360 Aldrich) before and after eclosion, grouped in vials according to sex, and aged for 10–14 days.
Flies were chilled on ice and decapitated under a low intensity of blue light (470 nm) and al-
362 lowed to recover for ~30 min before being transferred into behavioral chambers (diameter: 10
mm, height: 3 mm). The chambers were kept in darkness and placed above an LED panel that
364 provided infrared light (850 nm) for continuous illumination and photoactivation with red light
(635 nm). The intensity and pattern of red-light illumination were controlled by a customized
366 Arduino script. Light intensity was confirmed with an optical power meter (Thorlabs, PM160).
A camera (FLIR Blackfly S USB3, BFS-U3-31S4M-C) equipped with a long-pass filter (cut-on
368 wavelength of 800 nm; Thorlabs, FEL0800) was placed above the chamber and videos were rec-
orded at 55 fps with a resolution of 0.03 mm/pixel. Courtship and receptivity assays were con-
370 ducted using group- and singly-housed virgin females and males, respectively. Behavior assays
were done at 25°C under white light, ~1–2 hrs after the start of the subjective day. Individual fe-
372 males and naive males were loaded into behavioral chambers (diameter: 10 mm, height: 3 mm)
and recorded for 30 min using a Sony Vixia HFR700 video camera. Ovipositor extrusion was as-
374 sessed using mated females prepared 24 hrs before the assay by grouping 10 virgin females and
20 wild-type males in a vial. Mated females were chilled on ice and sorted 30 min before the as-
376 say. Individual females and naive Canton S males were loaded into behavioral chambers as de-
scribed above and video recorded for 15 min. For male abdominal curling measurements, virgin
378 Canton S females and experimental or control males were collected and housed as described
above. Virgin females were chilled on ice and decapitated to prevent copulation 30 min before
380 being transferred individually into behavioral chambers with a male. The pairs were recorded
for 15 min. Change in abdominal length was measured from frames before and during a vpo or
382 oe where the female was in the same position in the chamber. The vpo and abdominal curling
indices were calculated by dividing the amount of time the female opened her vaginal plates or
384 the male curled his abdomen by the total photoactivation time of each bout. Courtship index

was measured as the total amount of time the male spent performing any courtship behavior divided by the total observation time. All p-values were measured in Matlab.

Acknowledgements

We thank Y. Ding, J. Lillvis, and E. Preger-Ben Noon for helpful discussions, and A. McStravog for administrative assistance. DLS is an Investigator with Howard Hughes Medical Institute. TRS is supported by a grant from the National Science Foundation.

References

1. Billeter, J.-C., Rideout, E.J., Dornan, A.J., and Goodwin, S.F. (2006). Control of male sexual behavior in Drosophila by the sex determination pathway. Curr. Biol. *16*, R766–R776.
2. Manoli, D.S., Foss, M., Villella, A., Taylor, B.J., Hall, J.C., and Baker, B.S. (2005). Male-specific fruitless specifies the neural substrates of Drosophila courtship behaviour. Nature *436*, 395–400.
3. Demir, E., and Dickson, B.J. (2005). fruitless splicing specifies male courtship behavior in Drosophila. Cell *121*, 785–794.
4. Stockinger, P., Kvitsiani, D., Rotkopf, S., Tirin, L., and Dickson, B.J. (2005). Neural circuitry that governs Drosophila male courtship behavior. Cell *121*, 795–807.
5. Robinett, C.C., Vaughan, A.G., Knapp, J.M., and Baker, B.S. (2010). Sex and the single cell. II. There is a time and place for sex. PLoS Biol. *8*(5), e1000365.
6. Rideout, E.J., Dornan, A.J., Neville, M.C., Eadie, S., and Goodwin, S.F. (2010). Control of sexual differentiation and behavior by the doublesex gene in Drosophila melanogaster. Nat. Neurosci. *13*, 458–466.
7. Waterbury, J.A., Jackson, L.L., and Schedl, P. (1999). Analysis of the doublesex female protein in Drosophila melanogaster: Role in sexual differentiation and behavior and dependence on intersex. Genetics *152*(4), 1653–1667.
8. Shirangi, T.R., Taylor, B.J., and McKeown, M. (2006). A double-switch system regulates male courtship behavior in male and female Drosophila melanogaster. Nat. Genet. *38*, 1435–1439.
9. Kvitsiani, D., and Dickson, B.J. (2006). Shared neural circuitry for female and male sexual behaviours in Drosophila. Curr. Biol. *16*(10), R355–R356.
10. Shirangi, T.R., and McKeown, M. (2007). Sex in flies: What "body-mind" dichotomy? Dev. Biol. *306*, 10–19.
11. Villella, A., and Hall, J.C. (2008). Neurogenetics of Courtship and Mating in Drosophila. Adv. Genet. *62*, 67–184.
12. Finley, K.D., Taylor, B.J., Milstein, M., and McKeown, M. (1997). dissatisfaction, a gene involved in sex-specific behavior and neural development of Drosophila melanogaster. Proc. Natl. Acad. Sci. USA *94*(3), 913–918.

13. Finley, K.D., Edeen, P.T., Foss, M., Gross, E., Ghbeish, N., Palmer, R.H., Taylor, B.J., and McKeown, M. (1998). dissatisfaction encodes a tailless-like nuclear receptor expressed in a subset of CNS neurons controlling Drosophila sexual behavior. Neuron *21*, 1363–1374.
14. Choi, H.M.T., Schwarzkopf, M., Fornace, M.E., Acharya, A., Artavanis, G., Stegmaier, J., Cunha, A., and Pierce, N.A. (2018). Third-generation in situ hybridization chain reaction: multiplexed, quantitative, sensitive, versatile, robust. Development *145*(2), dev165753.
15. Choi, H.M.T., Beck, V.A., and Pierce, N.A. (2014). Next-Generation in Situ Hybridization Chain Reaction: Higher Gain, Lower Cost, Greater Durability. ACS Nano *8*(5), 4284–4294.
16. Choi, H.M.T., Chang, J.Y., Trinh, L.A., Padilla, J.E., Fraser, S.E., and Pierce, N.A. (2010). Programmable in situ amplification for multiplexed imaging of mRNA expression. Nat. Biotechnol. *28*, 1208–1212.
17. Court, R., Namiki, S., Armstrong, J.D., Börner, J., Card, G., Costa, M., Dickinson, M., Duch, C., Korff, W., Mann, R., *et al.* (2020). A Systematic Nomenclature for the Drosophila Ventral Nerve Cord. Neuron *107*, 1071-1079.e2.
18. Ito, K., Shinomiya, K., Ito, M., Armstrong, J.D., Boyan, G., Hartenstein, V., Harzsch, S., Heisenberg, M., Homberg, U., Jenett, A., *et al.* (2014). A systematic nomenclature for the insect brain. Neuron *81*, 755–765.
19. Zhou, C., Pan, Y., Robinett, C.C., Meissner, G.W., and Baker, B.S. (2014). Central brain neurons expressing doublesex regulate female receptivity in Drosophila. Neuron *83*, 149–163.
20. Klapoetke, N.C., Murata, Y., Kim, S.S., Pulver, S.R., Birdsey-Benson, A., Cho, Y.K., Morimoto, T.K., Chuong, A.S., Carpenter, E.J., Tian, Z., *et al.* (2014). Independent optical excitation of distinct neural populations. Nat. Methods *11*, 338–346.
21. Mezzera, C., Brotas, M., Gaspar, M., Pavlou, H.J., Goodwin, S.F., and Vasconcelos, M.L. (2020). Ovipositor Extrusion Promotes the Transition from Courtship to Copulation and Signals Female Acceptance in Drosophila melanogaster. Curr. Biol. *30*, 3736-3748.e5.
22. Wang, K., Wang, F., Forknall, N., Yang, T., Patrick, C., Parekh, R., and Dickson, B.J. (2021). Neural circuit mechanisms of sexual receptivity in Drosophila females. Nature *589*, 577–581.
23. Wang, F., Wang, K., Forknall, N., Parekh, R., and Dickson, B.J. (2020). Circuit and Behavioral Mechanisms of Sexual Rejection by Drosophila Females. Curr. Biol. *30*, 3749–3760.e3.
24. Kimura, K.I., Sato, C., Koganezawa, M., and Yamamoto, D. (2015). Drosophila ovipositor extension in mating behavior and Egg deposition involves distinct sets of brain interneurons. PLoS One *10*(5), e0126445.
25. Sweeney, S.T., Broadie, K., Keane, J., Niemann, H., and O'Kane, C.J. (1995). Targeted expression of tetanus toxin light chain in Drosophila specifically eliminates synaptic transmission and causes behavioral defects. Neuron *14*, 341–351.
26. Haley, B., Hendrix, D., Trang, V., and Levine, M. (2008). A simplified miRNA-based gene silencing method for Drosophila melanogaster. Dev. Biol. *321*, 482–490.
27. Shirangi, T.R., Wong, A.M., Truman, J.W., and Stern, D.L. (2016). Doublesex Regulates the Connectivity of a Neural Circuit Controlling Drosophila Male Courtship Song. Dev. Cell *37*, 533–544.

28. McKeown, M., Belote, J.M., and Boggs, R.T. (1988). Ectopic expression of the female transformer gene product leads to female differentiation of chromosomally male drosophila. Cell *53*, 887–895.
29. Pan, Y.F., Robinett, C.C., and Baker, B.S. (2011). Turning Males On: Activation of Male Courtship Behavior in Drosophila melanogaster. PLoS One *6*(6), e21144.
30. Shi, Y., Lie, D.C., Taupin, P., Nakashima, K., Ray, J., Yu, R.T., Gage, F.H., and Evans, R.M. (2004). Expression and function of orphan nuclear receptor TLX in adult neural stem cells. Nature *427*, 78–83.
31. Liu, H.K., Belz, T., Bock, D., Takacs, A., Wu, H., Lichter, P., Chai, M., and Schütz, G. (2008). The nuclear receptor tailless is required for neurogenesis in the adult subventricular zone. Genes Dev. *22*, 2473–2478.
32. Zhang, C.L., Zou, Y., He, W., Gage, F.H., and Evans, R.M. (2008). A role for adult TLX-positive neural stem cells in learning and behaviour. Nature *451*, 1004–1007.
33. Younossi-Hartenstein, A., Green, P., Liaw, G.J., Rudolph, K., Lengyel, J., and Hartenstein, V. (1997). Control of early neurogenesis of the Drosophila brain by the head gap genes tll, otd, ems, and btd. Dev. Biol. *182*, 270–283.
34. Mangelsdorf, D.J., and Evans, R.M. (1995). The RXR heterodimers and orphan receptors. Cell *83*, 841–850.
35. Pitman, J.L., Tsai, C.C., Edeen, P.T., Finley, K.D., Evans, R.M., and McKeown, M. (2002). DSF nuclear receptor acts as a repressor in culture and in vivo. Dev. Biol. *245*(2), 315–328.
36. Lee, J.W., Lee, Y.C., Na, S.Y., Jung, D.J., and Lee, S.K. (2001). Transcriptional coregulators of the nuclear receptor superfamily: Coactivators and corepressors. Cell. Mol. Life Sci. *58*, 289–297.
37. Hammer, G.D., Krylova, I., Zhang, Y., Darimont, B.D., Simpson, K., Weigel, N.L., and Ingraham, H.A. (1999). Phosphorylation of the nuclear receptor SF-1 modulates cofactor recruitment: Integration of hormone signaling in reproduction and stress. Mol. Cell *3*, 521–526.
38. Clough, E., Jimenez, E., Kim, Y.A., Whitworth, C., Neville, M.C., Hempel, L.U., Pavlou, H.J., Chen, Z.X., Sturgill, D., Dale, R.K., *et al.* (2014). Sex- and tissue-specific functions of drosophila doublesex transcription factor target genes. Dev. Cell *31*, 761–773.
39. Haley, B., Foys, B., and Levine, M. (2010). Vectors and parameters that enhance the efficacy of RNAi-mediated gene disruption in transgenic Drosophila. Proc. Natl. Acad. Sci. USA *107*, 11435–11440.
40. Gibson, D.G., Young, L., Chuang, R.-Y., Venter, J.C., Hutchison, C.A., and Smith, H.O. (2009). Enzymatic assembly of DNA molecules up to several hundred kilobases. Nat. Methods *6*, 343–345.
41. Port, F., Chen, H., Lee, T., and Bullock, S.L. (2014). Optimized CRISPR/Cas tools for efficient germline and somatic genome engineering in Drosophila. Proc. Natl. Acad. Sci. USA *111*(29), E2967–E2976.

Figure Legends

508 **Figure 1. Expression of *dsf* mRNA in the adult Drosophila central nervous system.** Confocal image of an adult Canton S female (a) and male (b) brain and VNC showing *dsf* mRNA expres-
510 sion labeled by *in situ* HCR using a probe-set directed against *dsf* transcripts. Hybridization signals are seen in several groups of cells in the brain and VNC. *dsf* mRNA expression was not de-
512 tected in the CNSs of females (c) and males (d) carrying partially overlapping deficiencies that delete the dsf gene. Scale bar represents 50 μm.

514

Figure 2. *dsf*^{Gal4} labels *dsf*-expressing neurons in the female and male adult central nervous
516 **system.** (a) Design of the *dsf*^{Gal4} allele. Targeted insertion of the Gal4 coding sequence (yellow box) after *dsf*'s translational start codon in exon 1 allows expression of Gal4 wherever dsf is nor-
518 mally expressed. Each box represents an exon. Exonic regions colored in light blue and white represent *dsf* coding sequences and untranslated regions, respectively. (b, c) Confocal images of
520 the adult brain, and third thoracic and abdominal ganglia of the VNC from *dsf*^{Gal4} > *UAS-nls::gfp* females (b) and males (c) showing co-localization of *dsf* mRNA (black) and GFP protein (green)
522 labeled by combined *in situ* HCR and immunohistochemistry. *dsf* mRNA and GFP protein expression overlap in the brain. GFP-expressing cells in the VNC exhibit *in situ* HCR signals, how-
524 ever some hybridization signals in the VNC lack GFP expression. These hybridization signals are likely non-specific to *dsf*, as they mostly persist in the VNCs of flies carrying deficiencies
526 that delete the *dsf* locus (see Figure 1c, d). Scale bar represents 50 μm. (d, e) Confocal images of brains and VNCs from *dsf*^{Gal4} > *UAS-nls::gfp* females (d) and males (e) showing the distribution
528 of GFP-expressing neurons in black and DNCad (neuropil) in light gray. Discrete groups of neurons were color-coded and categorized on one side of the brain according to standardized
530 nomenclatures. Neuronal groups that exhibit sex differences in neuron number are labeled in bold. (f) Table showing the average number of neurons in each *dsf*^{Gal4}-expressing neuronal
532 group in the brain and VNC of females and males. (g, h) Confocal images of brains and VNCs from *dsf*^{Gal4} > *UAS-myr::gfp* of females (g) and males (h) showing the projection and arborization
534 patterns of *dsf*^{Gal4}-expressing neurons in black and DNCad (neuropil) in light gray. Scale bar represents 50 μm.

536

Figure 3. A sexually dimorphic group of *dsf* and *dsx* co-expressing interneurons in abdominal
538 **ganglion.** The intersection of dsf^{Gal4} and $dsx^{LexA::p65}$ targets the sexually dimorphic DDAG neurons in the abdominal ganglion of females (a) and males (b). GFP-expressing neurons and DNCad
540 (neuropil) are shown in black and light gray, respectively. No other neurons are labeled by this intersection.

542

Figure 4. Activity of the DDAG neurons is sufficient and necessary for opening of the vagi-
544 **nal plates in females during courtship.** (a) A still frame image of a $dsf^{Gal4} \cap dsx^{LexA::p65}$ > *CsChrimson* virgin female, immobilized from decapitation, before (left) and after (right) illumi-
546 nation with 14.6 μW/mm^2 of red light to photoactivate the DDAG neurons. (b) The change in abdominal length upon an opening of the vaginal plates in virgin females and an ovipositor ex-
548 trusion in mated females was measured and compared to the change in abdominal length induced upon photoactivation of the DDAG neurons. (c) An ethogram of vaginal plate opening
550 behavior of nine $dsf^{Gal4} \cap dsx^{LexA::p65}$ > *CsChrimson* virgin females over the course of seven 15-sec bouts of photoactivation (red bars). (d, e) Fraction of time a virgin female opens her vaginal
552 plates during a 15-s bout of photoactivation (*i.e.*, the vpo index) and the change in abdominal length upon photoactivation (e) are largely unchanged across a variety of light intensities. (f–h)
554 Virgin females with inhibited DDAG neurons using tetanus neurotoxin (magenta) are unreceptive to active male courtship and exhibit a reduced frequency of vaginal plate opening behav-
556 iors relative to the control (black). (f) Fraction of virgin females that mated with a Canton S male over 30 minutes. (g) Fraction of time a Canton S male spent courting a virgin female during 5
558 minutes of observation (*i.e.*, courtship index). (h) Number of times a virgin female opened her vaginal plates per minute of active courtship by a Canton S male. (i, j) Depletion of *dsf* tran-
560 scripts in *dsx*-expressing neurons of females (magenta) results in reduced receptivity and frequency of vaginal plate opening behavior compared to controls (black and orange). (b), (d), (e),
562 (g), (h), (j) show individual points, mean, and SD. Significance was measured using one-way ANOVA with a Tukey-Kramer post hoc test for multiple comparisons. n.s., not significant. Sig-
564 nificance in (f) and (i) was measured using a log-rank test.

566 **Figure 5. Activity of the DDAG neurons is sufficient and necessary for abdominal curling during male courtship.** (a) A still frame image of a decapitated *dsf*^{Gal4} ∩ *dsx*$^{LexA::p65}$ > *CsChrimson*
568 male before (left) and after (right) illumination with 14.6 μW/mm^2 of red light to photoactivate the DDAG neurons. (b) An ethogram of abdominal curling of nine *dsf*^{Gal4} ∩ *dsx*$^{LexA::p65}$ >
570 *CsChrimson* males over the course of seven 15-sec bouts of photoactivation (red bars). (c) The fraction of time a *dsf*^{Gal4} ∩ *dsx*$^{LexA::p65}$ > *CsChrimson* male curls his abdomen (*i.e.*, abdominal curl-
572 ing index) during bouts of photoactivation (green) and darkness (black) in a dsf heterozygous (dsfGal4/+) and dsf mutant (*dsf*^{Gal4}/*dsf*^{Del}) background. (d–f) Males with inhibited DDAG neurons
574 using tetanus neurotoxin (magenta) exhibit reduced mating rates and frequency of abdominal curls per minute of active courtship relative to the control (black). (d) Fraction of males that
576 mated with a Canton S virgin female over 30 minutes. (e) Courtship index of males. (f) Number of abdominal curls per minute of active courtship. (g, h) Depletion of *dsf* transcripts in *dsx*-ex-
578 pressing neurons of males (magenta) results in reduced mating rates and frequency of abdominal curls compared to controls (black and orange). (c), (e), (f), and (h) show individual
580 points (i.e., individual females), mean, and SD. Significance was measured using one-way ANOVA with a Tukey-Kramer post hoc test for multiple comparisons. n.s., not significant. Sig-
582 nificance in (d) and (g) was measured using a log-rank test.

584 **Figure 6. *dsf* promotes and suppresses female-type development and function of the DDAG neurons depending upon the expression of *dsx*.** (a) The number of DDAG neurons per side in
586 *dsf* heterozygous (*dsf*^{Gal4}/+), *dsx* knock-down (*dsf*^{Gal4} > *UAS-dsx-ShmiR*), *dsf* mutant (*dsf*^{Gal4}/*dsf*^{Del}), and *dsx* knock-down, *dsf* mutant (*dsf*^{Gal4}/*dsf*^{Del} > *UAS-dsx-ShmiR*) females (black) and males (ma-
588 genta). The DDAG neurons were visualized in *dsf*^{Gal4} ∩ *dsx*$^{LexA::p65}$ > *myr::gfp* flies. (b–i) Exemplary confocal images of VNCs from the four genotypes analyzed in (a). (j) A still frame image
590 of a decapitated *dsf*^{Gal4} > *UAS-dsx-ShmiR* virgin female before (left) and after (right) photoactivation of the DDAG neurons with 14.6 μW/mm^2 of red light. (k) The vpo index of virgin females
592 expressing CsChrimson in the DDAG neurons during darkness (black) and during 15-s bouts of photoactivation (green). The vpo index was measured in *dsf* heterozygous (*dsf*^{Gal4}/+), *dsx*

594 knock-down (*dsf*^{Gal4} > *UAS-dsx-ShmiR*), *dsf* mutant (*dsf*^{Gal4}/*dsf*^{Del}), and *dsx* knock-down, *dsf* mutant (*dsf*^{Gal4}/*dsf*^{Del} > *UAS-dsx-ShmiR*) females. *dsf*^{Gal4} ∩ *dsx*$^{LexA::p65}$ was used to target the expression
596 *CsChrimson* in the DDAG neurons. (l) A still frame image of a decapitated *dsf*^{Gal4} > *UAS-dsx-ShmiR* male before (left) and after (right) photoactivation of the DDAG neurons with 14.6
598 μW/mm^2 of red light. Photoactivation of the DDAG neurons in males with depleted *dsx*M transcripts results in an extrusion of the male's terminalia. (m) The fraction of time a male express-
600 ing *CsChrimson* in the DDAG neurons exhibits a terminalia extrusion (*i.e.*, te index) during darkness (black) and during 15-s bouts of photoactivation (green). (a), (k), and (m) show individual
602 points, mean, and SD. Significance (P<0.05) was measured using one-way ANOVA with a Tukey-Kramer post hoc test for multiple comparisons. Same letter denotes no significant differ-
604 ence.

606 **Supplemental Figure 1.** *dsf*^{Gal4} CNS expression during larval and pupal life (a–d) *dsf*^{Gal4}-labeled cells in the CNS of females and males express the neuronal marker, ELAV. (e–f) *dsf*^{Gal4} labels
608 neurons in the late third instar larval female and male CNS. (g–j) *dsf*^{Gal4} labels CNS neurons in females and males during pupal life.

610

Supplemental Figure 2. Ectopic expression of *tra*F in the DDAG neurons feminizes the anatomy
612 and function of the DDAG neurons. (a) Ectopic expression of *tra*F driven by *dsf*^{Gal4} feminizes the anatomy of the DDAG neurons in males. (b) Photoactivation of the DDAG neurons in *dsf*^{Gal4} >
614 *UAS-traF* males induces terminalia extrusion behavior.

616 **Supplemental Video 1.** Optogenetic activation of DDAG neurons in *dsf*^{Gal4}/+ females. Photoactivation period begins with the green dot.
618 **Supplemental Video 2.** Optogenetic activation of DDAG neurons in *dsf*^{Gal4}/+ males.
Supplemental Video 3. Optogenetic activation of DDAG neurons in *dsf*^{Gal4} > *UAS-dsx-ShmiR* fe-
620 males.
Supplemental Video 4. Optogenetic activation of DDAG neurons in *dsf*^{Gal4} > *UAS-dsx-ShmiR*
622 males.

Supplemental Video 5. Optogenetic activation of DDAG neurons in *dsf*^{Gal4}/*dsf*^{Del} females.

624 **Supplemental Video 6.** Optogenetic activation of DDAG neurons in *dsf*^{Gal4}/*dsf*^{Del} males.

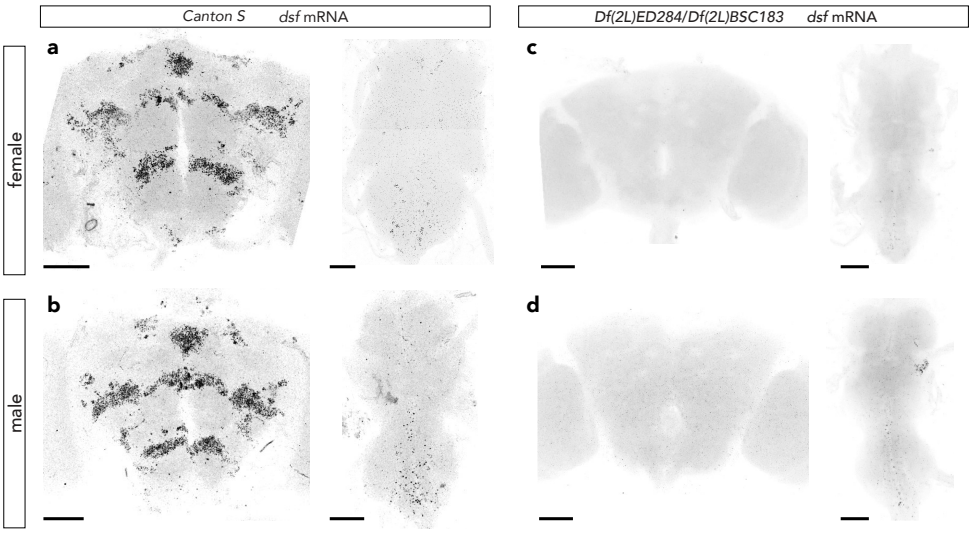

Figure 1. Expression of *dsf* mRNA in the adult Drosophila central nervous system. Confocal image of an adult Canton S female (a) and male (b) brain and VNC showing dsf mRNA expression labeled by *in situ* HCR using a probe-set directed against *dsf* transcripts. Hybridization signals are seen in several groups of cells in the brain and VNC. *dsf* mRNA expression was not detected in the CNSs of females (c) and males (d) carrying partially overlapping deficiencies that delete the *dsf* gene. Scale bar represents 50 μm.

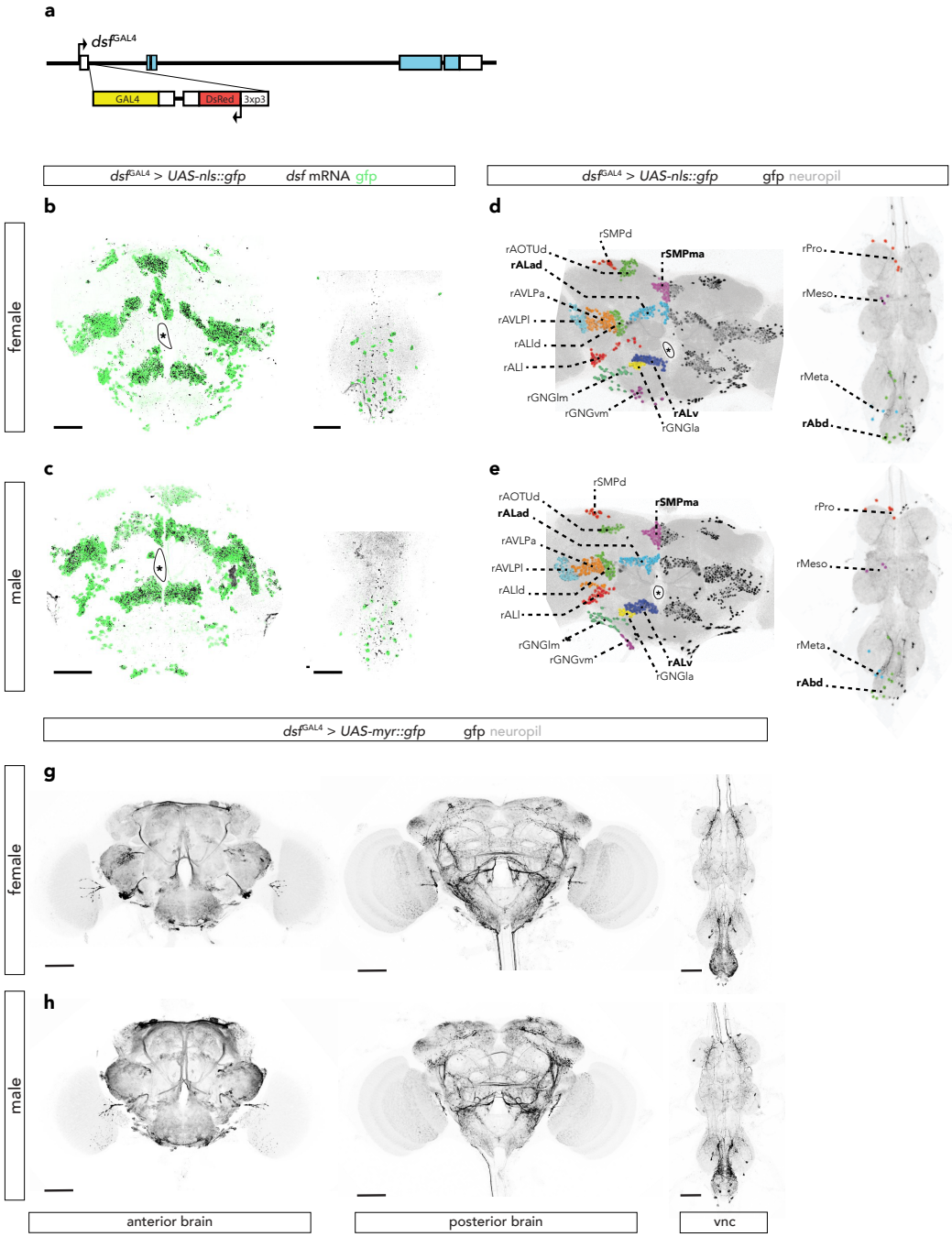

			female	male
brain	supraesophageal	rSMPd	10.5±1	11±1.8
		rSMPma	57±10	76±3
		rAOTUd	45±6	49±5
		rALad	54±4.5	92±5
		rAVLPa	60±12	70±12
		rAVLPl	60.5±12	62±19
		rALld	52.5±10	57±5
		rALl	36.5±6	31±4
	subesophageal	rGNGlm	24±6	26±6
		rGNGvm	9.75±0.5	9±0.5
		rALv	77±7.5	106±4
		rGNGla	42.5±7	48.5±6
ventral nerve cord	thoracic	rPro	6.5±1	6±0.5
		rMeso	2.9±0.8	2.9±0.3
		rMeta	4.1±0.3	3.75±0.5
		rAbd	15±2	8.75±1

Figure 2. *dsf*^{Gal4} labels *dsf*-expressing neurons in the female and male adult central nervous system. (a) Design of the *dsf*^{Gal4} allele. Targeted insertion of the Gal4 coding sequence (yellow box) after dsf's translational start codon in exon 1 allows expression of Gal4 wherever *dsf* is normally expressed. Each box represents an exon. Exonic regions colored in light blue and white represent *dsf* coding sequences and untranslated regions, respectively. (b, c) Confocal images of the adult brain, and third thoracic and abdominal ganglia of the VNC from *dsf*^{Gal4} > UAS-nls::gfp females (b) and males (c) showing co-localization of *dsf* mRNA (black) and GFP protein (green) labeled by combined *in situ* HCR and immunohistochemistry. *dsf* mRNA and GFP protein expression overlap almost perfectly in the brain. GFP-expressing cells in the VNC exhibit *in situ* HCR signals, however some hybridization signals in the VNC lack GFP expression. These hybridization signals are likely non-specific to dsf, as they mostly persist in the VNCs of flies carrying deficiencies that delete the *dsf* locus (see Figure 1c, d). Scale bar represents 50 µm. (d, e) Confocal images of brains and VNCs from *dsf*^{Gal4} > UAS-nls::gfp females (d) and males (e) showing the distribution of GFP-expressing neurons in black and DNCad (neuropil) in light gray. Discrete groups of neurons were color-coded and categorized on one side of the brain according to standardized nomenclatures. Neuronal groups that exhibit sex differences in neuron number are labeled in bold. (f) Table showing the average number of neurons in each *dsf*^{Gal4}-expressing neuronal group in the brain and VNC of females and males. (g, h) Confocal images of brains and VNCs from *dsf*^{Gal4} > UAS-myr::gfp of females (g) and males (h) showing the projection and arborization patterns of *dsf*^{Gal4}-expressing neurons in black and DNCad (neuropil) in light gray. Scale bar represents 50 µm.

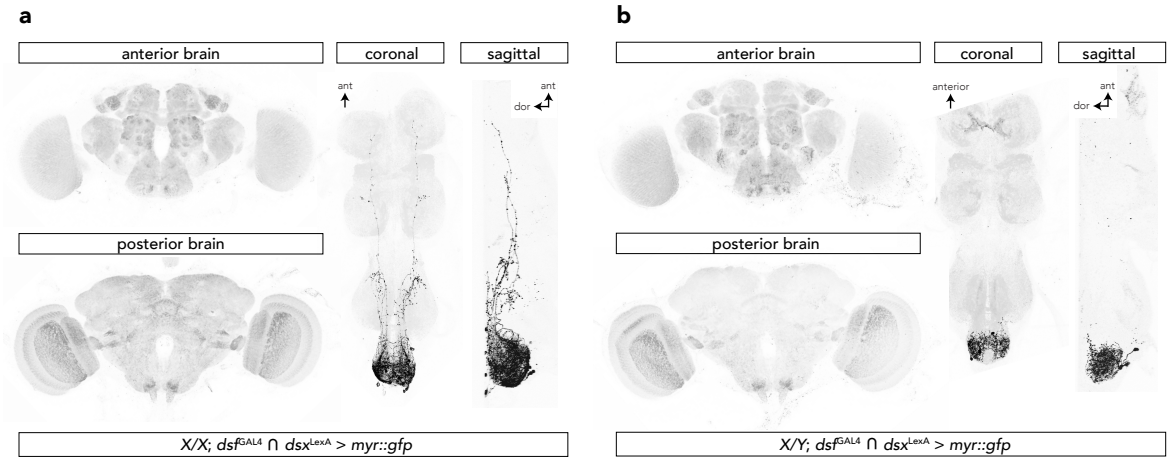

Figure 3. A sexually dimorphic group of *dsf* and *dsx* co-expressing interneurons in abdominal ganglion. The intersection of *dsf*^{Gal4} and *dsx*$^{LexA::p65}$ targets the sexually dimorphic DDAG neurons in the abdominal ganglion of females (a) and males (b). GFP-expressing neurons and DNCad (neuropil) are shown in black and light gray, respectively. No other neurons are labeled by this intersection.

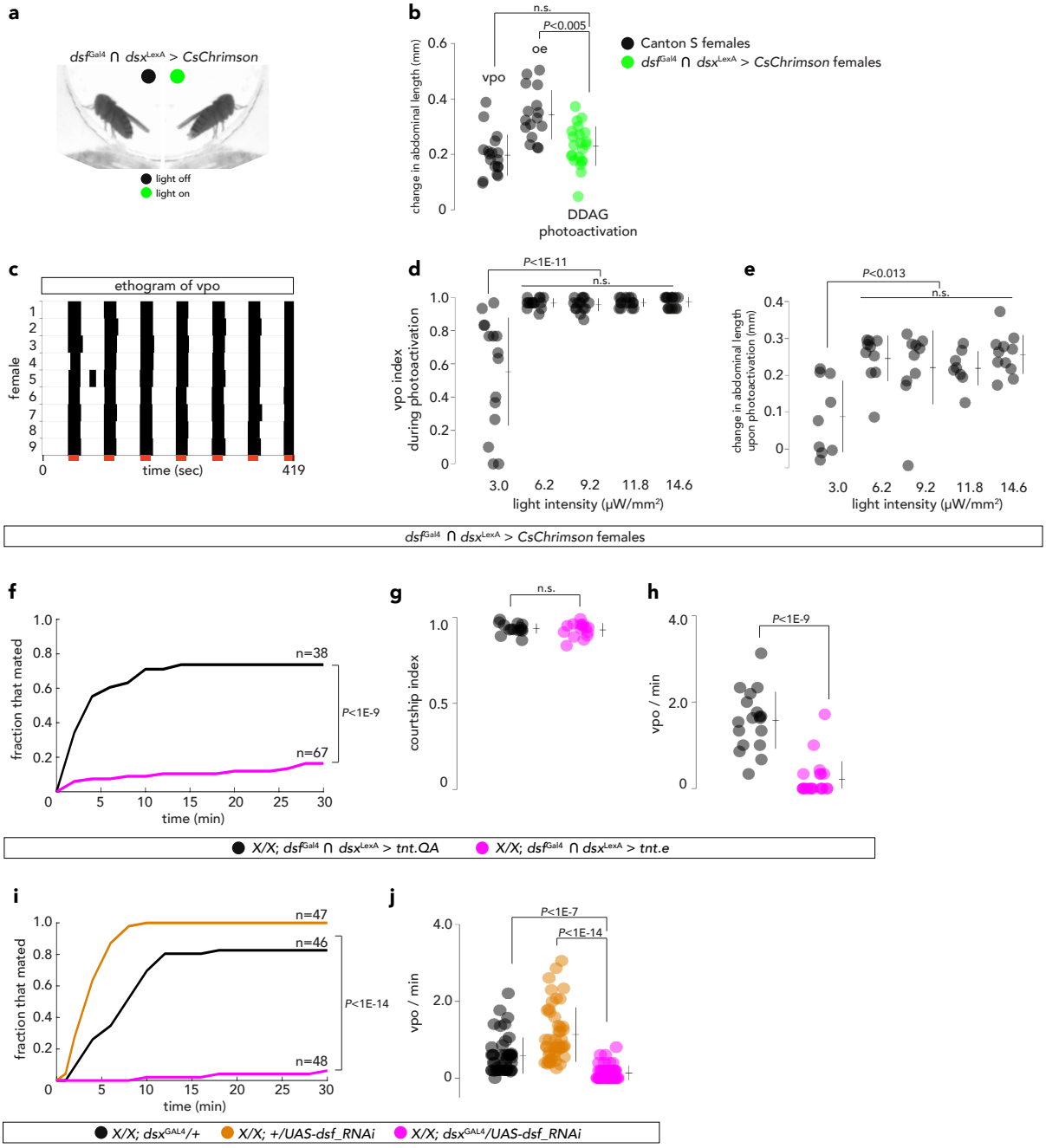

Figure 4. Activity of the DDAG neurons is sufficient and necessary for opening of the vaginal plates in females during courtship. (a) A still frame image of a decapitated *dsf*^{Gal4} *dsx*$^{LexA::p65}$ > CsChrimson virgin female before (left) and after (right) illumination with 14.6 μW/mm^2 of red light to photoactivate the DDAG neurons. (b) The change in abdominal length upon an opening of the vaginal plates in virgin females and an ovipositor extrusion in mated females was measured and compared to the change in abdominal length induced upon photoactivation of the DDAG neurons. (c) An ethogram of vaginal plate opening behavior of nine *dsf*^{Gal4} *dsx*$^{LexA::p65}$ > CsChrimson virgin females over the course of seven 15-sec bouts of photoactivation (red bars). (d, e) Fraction of time a virgin female opens her vaginal plates during a 15-s bout of photoactivation (i.e., the vpo index) and the change in abdominal length upon photoactivation (e) are largely unchanged across a variety of light intensities. (f–h) Virgin females with inhibited DDAG neurons using tetanus neurotoxin (magenta) are unreceptive to active male courtship and exhibit a reduced frequency of vaginal plate opening behaviors relative to the control (black). (f) Fraction of virgin females that mated with a Canton S male over 30 minutes. (g) Fraction of time a Canton S male spent courting a virgin female during 5 minutes of observation (i.e., courtship index). (h) Number of times a virgin female opened her vaginal plates per minute of active courtship by a Canton S male. (i, j) Depletion of *dsf* transcripts in *dsx*-expressing neurons of females (magenta) results in reduced receptivity and frequency of vaginal plate opening behavior compared to controls (black and orange). (b), (d), (e), (g), (h), (j) show individual points, mean, and SD. Significance was measured using one-way ANOVA with a Tukey-Kramer post hoc test for multiple comparisons. n.s., not significant. Significance in (f) and (i) was measured using a log-rank test.

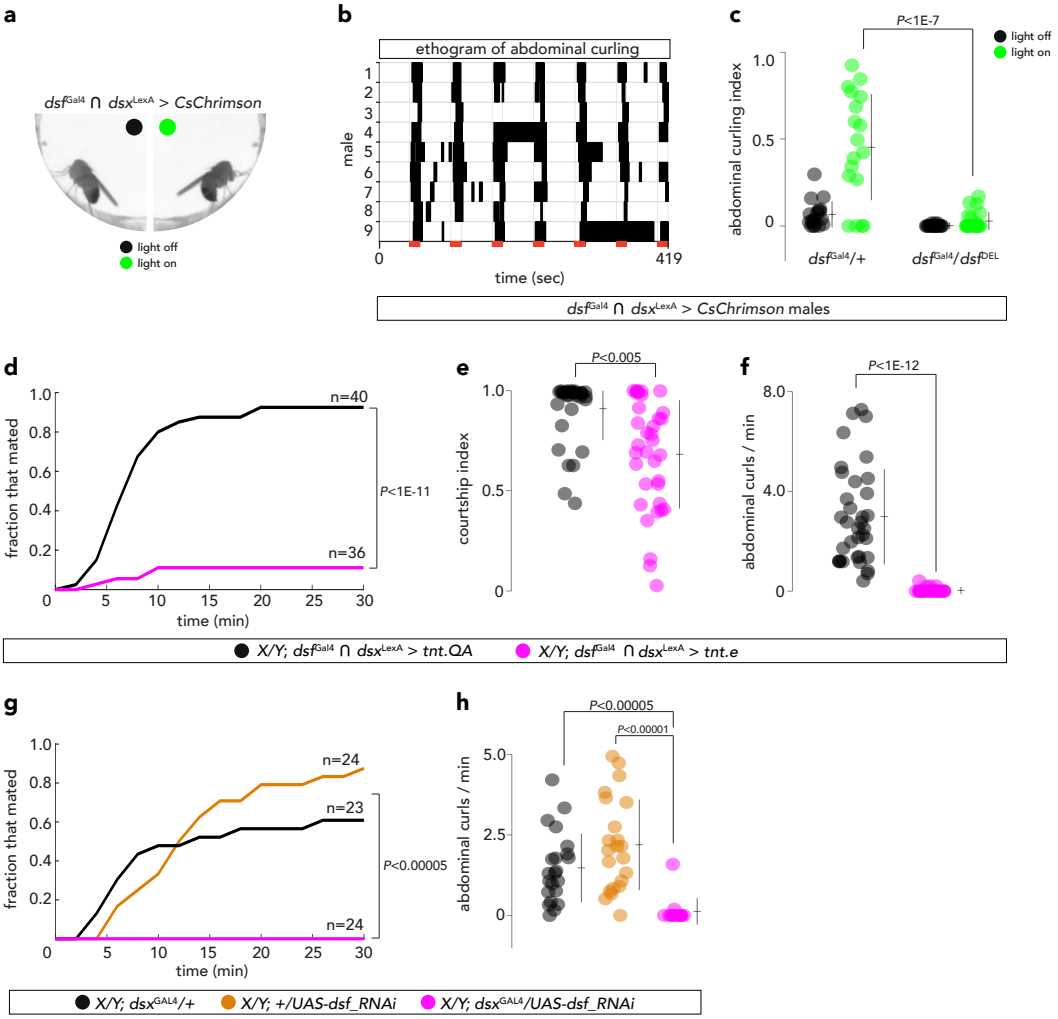

Figure 5. Activity of the DDAG neurons is sufficient and necessary for abdominal curling during male courtship. (a) A still frame image of a decapitated *dsf*^{Gal4} *dsx*$^{LexA::p65}$ > CsChrimson male before (left) and after (right) illumination with 14.6 μW/mm^2 of red light to photoactivate the DDAG neurons. (b) An ethogram of abdominal curling of nine *dsf*^{Gal4} *dsx*$^{LexA::p65}$ > CsChrimson males over the course of seven 15-sec bouts of photoactivation (red bars). (c) The fraction of time a *dsf*^{Gal4} *dsx*$^{LexA::p65}$ > CsChrimson male curls his abdomen (i.e., abdominal curling index) during bouts of photoactivation (green) and darkness (black) in a *dsf* heterozygous (*dsf*^{Gal4}/+) and *dsf* mutant (*dsf*^{Gal4}/*dsf*^{DEL}) background. (d–f) Males with inhibited DDAG neurons using tetanus neurotoxin (magenta) exhibit reduced mating rates and frequency of abdominal curls per minute of active courtship relative to the control (black). (d) Fraction of males that mated with a Canton S virgin female over 30 minutes. (e) Courtship index of males. (f) Number of abdominal curls per minute of active courtship. (g, h) Depletion of *dsf* transcripts in *dsx*-expressing neurons of males (magenta) results in reduced mating rates and frequency of abdominal curls compared to controls (black and orange). (c), (e), (f), and (h) show individual points (i.e., individual females), mean, and SD. Significance was measured using one-way ANOVA with a Tukey-Kramer post hoc test for multiple comparisons. n.s., not significant. Significance in (d) and (g) was measured using a log-rank test.

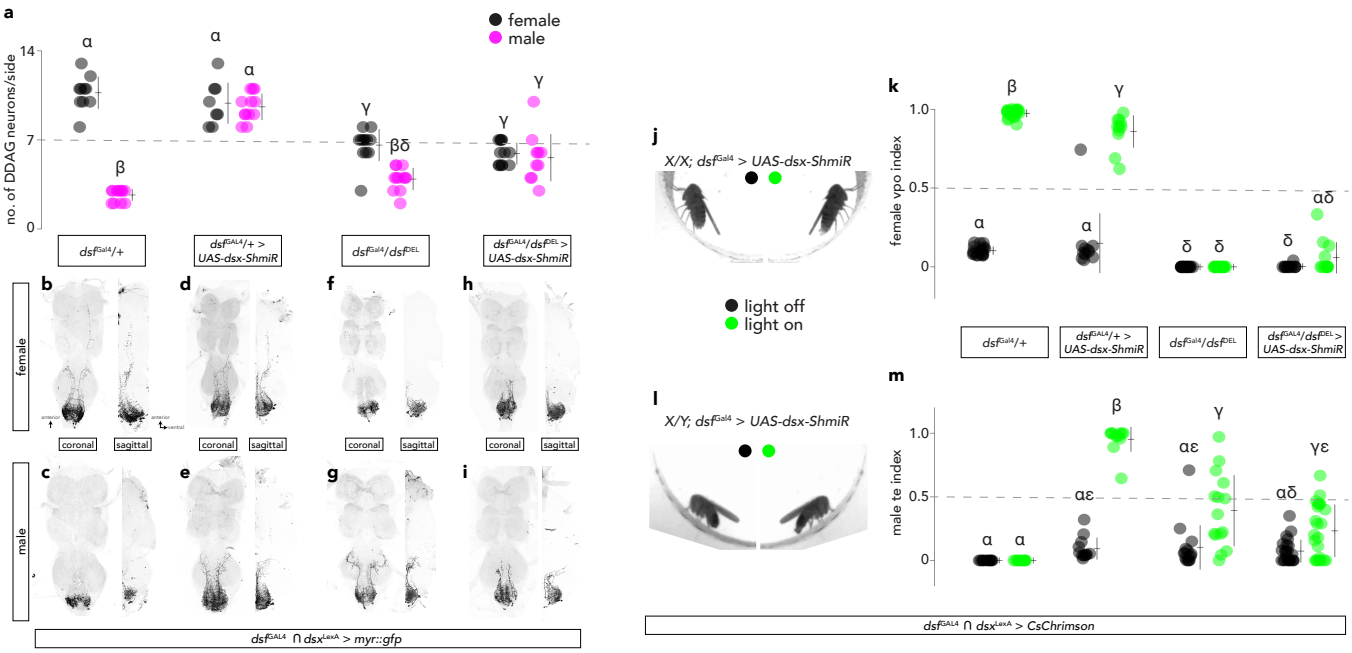

Figure 6. *dsf* promotes and suppresses female-type development and function of the DDAG neurons depending upon the expression of *dsx*. (a) The number of DDAG neurons per side in *dsf* heterozygous (dsf^{Gal4}/+), *dsx* knock-down (dsf^{Gal4} > UAS-dsx-ShmiR), *dsf* mutant (dsf^{Gal4}/dsf^{DEL}), and *dsx* knock-down, *dsf* mutant (dsf^{Gal4}/dsf^{DEL} > UAS-dsx-ShmiR) females (black) and males (magenta). The DDAG neurons were visualized in dsf^{Gal4} $dsx^{LexA::p65}$ > myr::gfp flies. (b–i) Confocal images of VNCs from the four genotypes analyzed in (a). (j) A still frame image of a decapitated dsf^{Gal4} > UAS-dsx-ShmiR virgin female before (left) and after (right) photoactivation of the DDAG neurons with 14.6 μW/mm2 of red light. (k) The vpo index of virgin females expressing CsChrimson in the DDAG neurons during darkness (black) and during 15-s bouts of photoactivation (green). The vpo index was measured in *dsf* heterozygous (dsf^{Gal4}/+), *dsx* knock-down (dsf^{Gal4} > UAS-dsx-ShmiR), *dsf* mutant (dsf^{Gal4}/dsf^{DEL}), and *dsx* knock-down, *dsf* mutant (dsf^{Gal4}/dsf^{DEL} > UAS-dsx-ShmiR) females. dsf^{Gal4} $dsx^{LexA::p65}$ was used to target the expression CsChrimson in the DDAG neurons. (l) A still frame image of a decapitated dsf^{Gal4} > UAS-dsx-ShmiR male before (left) and after (right) photoactivation of the DDAG neurons with 14.6 μW/mm^2 of red light. Photoactivation of the DDAG neurons in males with depleted *dsx*M transcripts results in an extrusion of the male's terminalia. (m) The fraction of time a male expressing CsChrimson in the DDAG neurons exhibits a terminalia extrusion (i.e., te index) during darkness (black) and during 15-s bouts of photoactivation (green). (a), (k), and (m) show individual points, mean, and SD. Significance (P<0.05) was measured using one-way ANOVA with a Tukey-Kramer post hoc test for multiple comparisons. Same letter denotes no significant difference.